Needle Propagation and Twinkling Characteristics

B. M. Hare[1], O. Scholten[1,2], J. Dwyer[3], C. Strepka[3], S. Buitink[4,5], A. Corstanje[4,5], H. Falcke[4,6,7], J.R. Hörandel[4,5,6], T. Huege[5,8], G. K. Krampah[5], P. Mitra[5], K. Mulrey[5], A. Nelles[9,10], H. Pandya[5], J. P. Rachen[5], S. Thoudam[11], T. N. G. Trinh[12], S. ter Veen[4,7], and T. Winchen[13]

[1]Kapteyn Astronomical Institute, University of Groningen, P.O. Box 72, 9700 AB Groningen, Netherlands
[2]Interuniversity Institute for High-Energy, Vrije Universiteit Brussel, Pleinlaan 2, 1050 Brussels, Belgium
[3]Department of Physics and Astronomy, University of New Hampshire, Durham, NH, USA
[4]Department of Astrophysics/IMAPP, Radboud University Nijmegen, P.O. Box 9010, 6500 GL Nijmegen, Netherlands
[5]Astrophysical Institute, Vrije Universiteit Brussel, Pleinlaan 2, 1050 Brussels, Belgium
[6]NIKHEF, Science Park Amsterdam, 1098 XG Amsterdam, Netherlands
[7]Netherlands Institute of Radio Astronomy (ASTRON), Postbus 2, 7990 AA Dwingeloo, Netherlands
[8]Institute for Astroparticle Physics (IAP), Karlsruhe Institute of Technology (KIT), P.O. Box 3640, 76021, Karlsruhe, Germany
[9] DESY, Platanenallee 6, 15738 Zeuthen, Germany
[10] ECAP, Friedrich-Alexander-University Erlangen-Nrnberg, 91058 Erlangen, Germany
[11]Department of Physics, Khalifa University, PO Box 127788, Abu Dhabi, United Arab Emirates
[12]Department of Physics, School of Education, Can Tho University Campus II, 3/2 Street, Ninh Kieu District, Can Tho City, Vietnam
[13]Max-Planck-Institut für Radioastronomie, P.O. Box 20 24, Bonn Germany

Key Points:

- Detailed distributions of needle properties are presented
- Possible physics behind needle production is discussed
- Recoil leaders quench needle activity

Corresponding author: B. M. Hare, B.H.Hare@rug.nl

Abstract

Recently, a new lightning phenomena, termed needles, has been observed in both VHF and in optical along positive lightning leaders. They appear as small (<100 m) leader branches that undergo dielectric breakdown at regular intervals (called twinkles). Providing a coherent and consistent explanation for this phenomenon is challenging as each twinkle is a form of negative breakdown that propagates away from the positive leader. In this work we provide detailed observations of needles in VHF, observed during two lightning flashes. We show distributions of different needle properties, including twinkle propagation speeds, time between twinkles, and needle lengths, among others. We show a return stroke and multiple recoil leaders that quench needle activity. We also show that nearby needle activity does not seem to correlate together, and that needle twinkling can slow down by 10 to 30 percent per twinkle. We conclude by presenting possibilities for how the positive leader could induce negative propagation away from the positive channel, and we argue that twinkles can propagate like a stepped leader or like a recoil leader depending on the temperature of the needle, which implies that needle twinkles can probably propagate without emitting VHF.

1 Introduction

Needles are a very recently discovered lightning phenomenon, described in B. Hare et al. (2019), that occur along positive leader channels. They appear like small leader branches, at most around 100 m long, and stick out from the channel. However, unlike leader branches, they exhibit ionization fronts that propagate up each needle, away from the positive leader channel. B. Hare et al. (2019) referred to these fronts as twinkles, and they occur at a very regular rate, around once per 5 ms. Pu and Cummer (2019) confirmed these findings, and showed that needle twinkles have a production head that moves forward along the positive at a regular speed, where there is no needle activity ahead of this head, and copious needle activity behind it.

Paradoxically, despite propagating away from the positive leader channel, B. Hare et al. (2019) concluded that since needles emit copious VHF while positive leaders do not (B. Hare et al., 2019; Edens et al., 2012; Shao et al., 1999), needle twinkles must thus be a form of negative propagation. Pu and Cummer (2019) confirmed this by showing

that the negatively charged end of a bi-leader suppressed needle activity, and by showing a needle that extended into a full negative leader.

Saba et al. (2020) was able to observe optical emissions from needles on upward positive leaders. Saba et al. (2020) showed that these needles observed in optical had very similar properties to those reported in B. Hare et al. (2019) and Pu and Cummer (2019), including that they twinkled multiple times with a few milliseconds between twinkles without growing in length. However, the needles observed by Saba et al. (2020) were somewhat shorter than those observed in B. Hare et al. (2019) and Pu and Cummer (2019). Saba et al. (2020) was even able to show that propagation of one 73 m long needle was away from the positive leader with a speed of about 2.7×10^5 m/s, and that a negative leader developed from the location of a needle, consistent with B. Hare et al. (2019) and Pu and Cummer (2019), and Saba et al. (2020) was able to confirm a hypothesis proposed by B. Hare et al. (2019), that the first needle twinkle occurs about 100 m or so behind the tip of the positive leader. Finally, Saba et al. (2020) was also able to show that needles are the result of a corona brush split, which is where the corona in front of a positive leader splits into two different sections in a failed attempt to branch.

In this work we present of observations of typical needle behavior during two lightning flashes, including statistics on their lengths, twinkling rates, propagation speeds, and more. Among others, we show that: needle twinkles can potentially propagate without emitting VHF radiation, have a wide range of propagation speeds varying from stepped leaders up to dart leaders, and that needles cease twinkling after recoil leaders. In section 2 we introduce the two flashes used in this work. In section 2.1 we discuss a needle from each flash in detail. In section 2.2 we give detailed statistics for many needles. In section 2.3 we explore the relationship between negative leader and needles, and in section 2.4 we explore the relation between recoil leaders and needles. In section 2.5 we discuss the broader structure of needle activity on the positive leader. Finally, in section 3, we discuss the possible physics behind needle twinkling and propagation.

2 Data

In this work we use two flashes observed by the Low Frequency ARray (LOFAR) (van Haarlem et al., 2013). For consistency we use the same flash presented in B. Hare et al. (2019), which was observed on 29, September, 2017 at 20:22:55 UTC. For compar-

ison we also include data from 24, April, 2019 at 19:44:32 UTC. We observed multiple flashes on this day, in this work we focus on one flash in particular, chosen because it is at the most optimal location for imaging (close enough that we have meter-scale accuracy, but not so close that the confusion limit becomes too large). The maps for both flashes are shown in Figure 1

Both of these flashes were imaged using a new algorithm that is improved over the one used in B. Hare et al. (2019), as it is significantly faster and locates around three times more sources. This new algorithm was inspired by Kalman-filters and is described in Scholten et al. (2020).

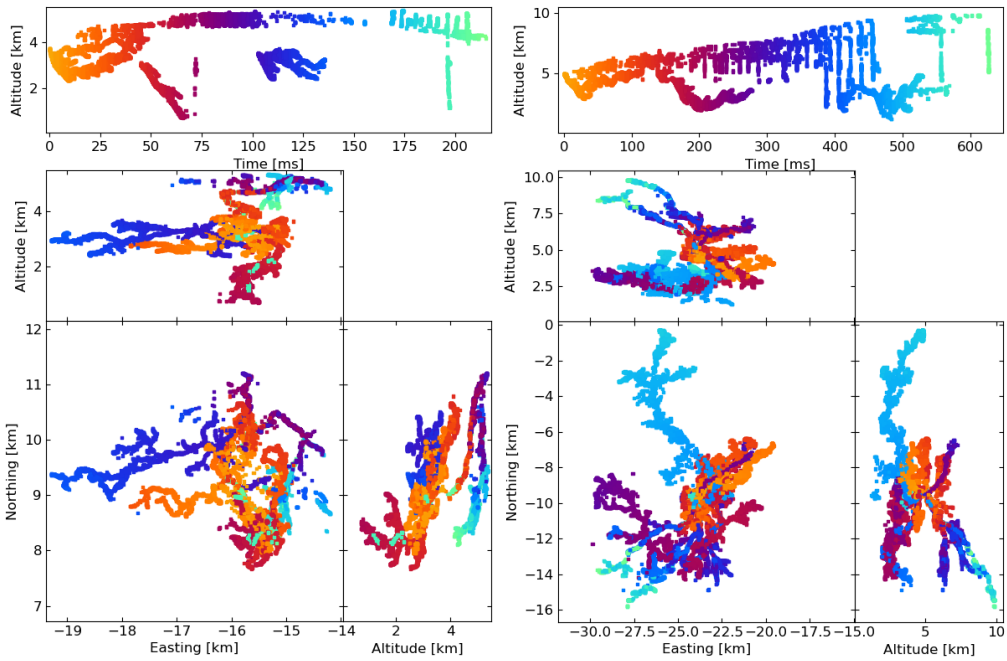

Figure 1. The maps of the two lightning flashes used in this work. The 2017 flash is on the left, and the 2019 flash is on the right. Both of these flashes propagate into the main negative charge and and the lower positive charge. Thus, each flash has two layers. The 2017 flash connects to ground and produces a return stroke at about 72 ms.

2.1 Specific Examples

Figure 2 shows two needles, one from each flash, that show the general characteristics of needles. For these two examples we purposely choose needles that are particularity long, as it is easier to demonstrate their important features. Furthermore, the

needle from 2017 was also featured in B. Hare et al. (2019), however here we see more detail due to the improved imaging procedure.

Figure 2 shows a straight line that has been fitted to the VHF source locations, which we call the axis. In Section 2.2 we fit this axis to a large number of needles in order to extract distributions of length, speed, and other characteristics. This fitting was done by modeling each twinkle as a point that moved forward along the axis. The direction and location of the axis was held to be the same for every twinkle in a needle, but each twinkle had a different fitted speed. The direction, location of the axis, and speed of each twinkle, was extracted by minimizing the distance between this front and each VHF source using a Levenberg-Marquardt optimizer.

In the distance along axis vs time panel of figure 2 each twinkle of the two needles appears as a vertical bar as the duration of each twinkle is much shorter than the time between twinkles. Each needle twinkles multiple times, with the time between twinkles generally around 5-10 ms. It is clear that the needles are not perfectly straight, they tend to curve, and each twinkle follows the same curved path. Furthermore, each twinkle does not extend the needle but also does not necessarily produce mappable VHF emission over the entire needle.

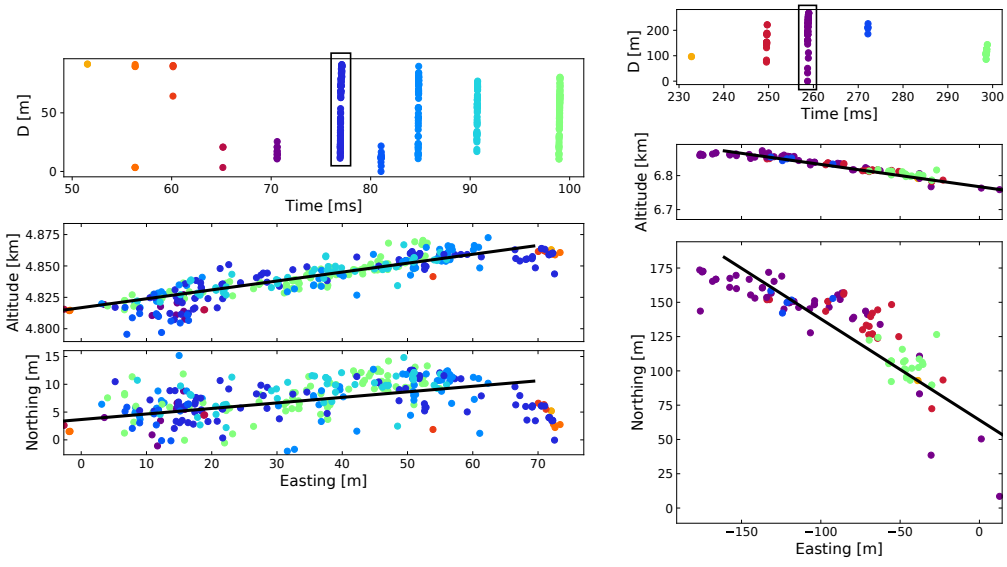

Figure 2. Examples of two needles. Black line shows the fitted axis. D is distance parallel to the axis. X=0 and Y=0 has been shifted. The rectangles in D vs T indicate the twinkles features in figure 3. The Left is 2017, right is 2019 flashes.

Figure 3 shows a zoom-in on a twinkle with many VHF sources from the two needles shown in figure 2 at T=77 ms and T=259 ms from the 2017 and 2019 flashes respectively. These two twinkles propagate at about 5.3×10^5 m/s and 9.2×10^5 m/s on average, respectively, away from the positive leader. It is interesting to compare these two twinkles to the one at about T=56 ms in the 2017 needle in figure 2, which simply consists of two clusters of sources at the base and tip of the 2017 needle, 86 m and 5.6 μs apart, thus propagated at a speed of 1.5×10^7 m/s, 30 times faster than the twinkles featured in figure 3. Both of the twinkles shown in figure 3, however, seem to start with a fast propagation and then slow down. We have observed many twinkles that slow down(such as these two), and many that seem to have a constant speed.

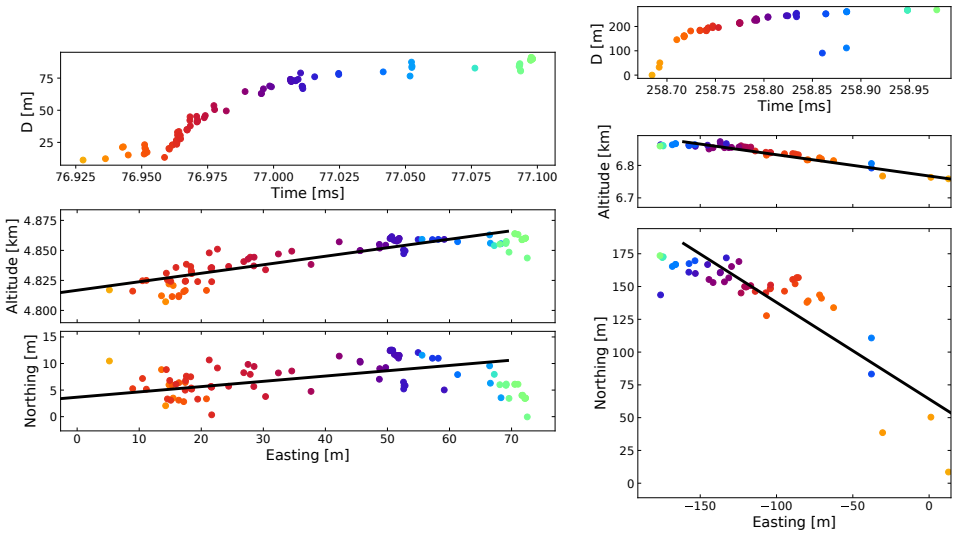

Figure 3. Examples of twinkles, in the needle shown in Figure 2. Left is 2017, right is 2019 flashes.

2.2 Statistical Characteristics

Figure 4 shows a distribution of number of twinkles per needle and figure 5 shows the distribution of time between twinkles per needle. These statistics were formed by choosing needles that could clearly be distinguished from other lightning structures (such as recoil leaders and other needles) using rectangular cuts in space and time, and twinkled at least twice, where a twinkle could consist of a single VHF source. The twinkles inside of each needle were separated when two subsequent VHF sources inside the same

needle were greater than 0.5 ms apart. We verified by eye that this cut produces good results for all needles used in this work. It is possible that these distributions are affected by imaging inefficiencies, as some twinkles emit very little VHF radiation (such as the first twinkle in the featured 2017 needle) and could be easily missed during imaging.

Figure 4 shows that the number of twinkles per needle follows a roughly uniform distribution, that there isn't one preferred number of twinkles. Figure 4 also shows that the maximum number of twinkles per needle is smaller in the 2019 flash than the 2017 flash. It is not clear if this is physical or due to imaging artifacts. Figure 5 shows that the time between twinkles tends to be between 2-7 ms. Large measured time between twinkles, especially larger than 10 ms, is most likely due to twinkles that were missed by the imaging.

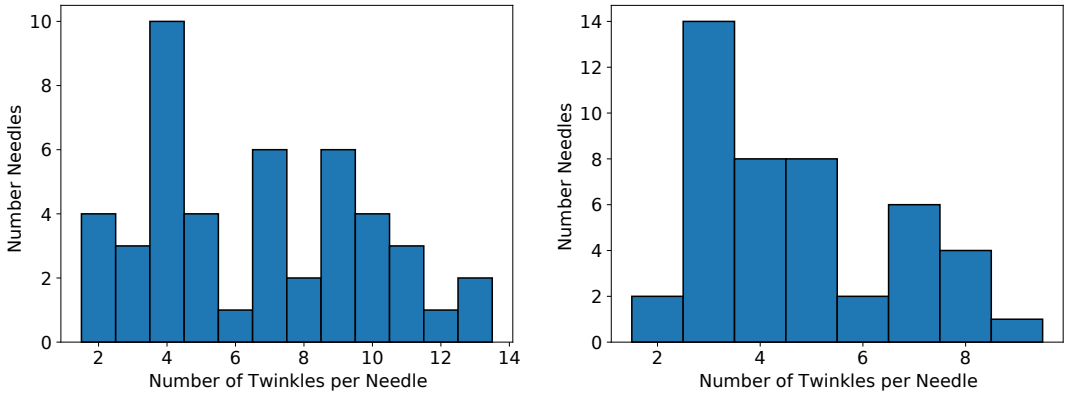

Figure 4. Number of twinkles per needle. Left is 2017, right is 2019 flashes.

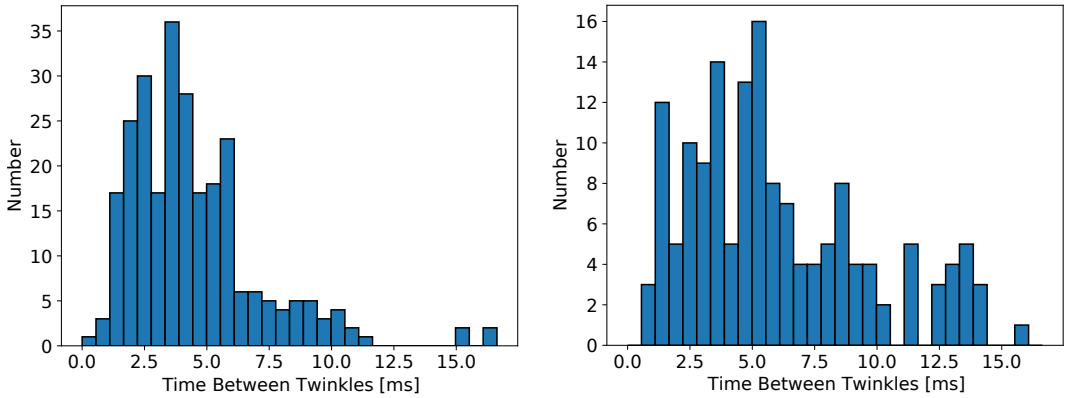

Figure 5. Histogram of the times between subsequent twinkles. Left is 2017, right is 2019 flashes.

The time between twinkles is very regular, as opposed to a random rate. Figure 6 shows the ratio of times between subsequent twinkles. I.E, if a needle has three twinkles, A, B, and C, and T_{AB} and T_{BC} is the time between twinkles A,B and B,C respectively, the distribution of T_{AB}/T_{BC} is shown in figure 6. Figure 6 also shows the results of a simple monte-carlo simulation that demonstrates how the results would appear if twinkling times were uncorrelated. This simulation was performed by simply sampling two values (with replacement) from the distribution of twinkling times, shown in figure 5, and taking their ratio. The difference between this simulation and the data demonstrates the strength of the correlation between subsequent twinkles.

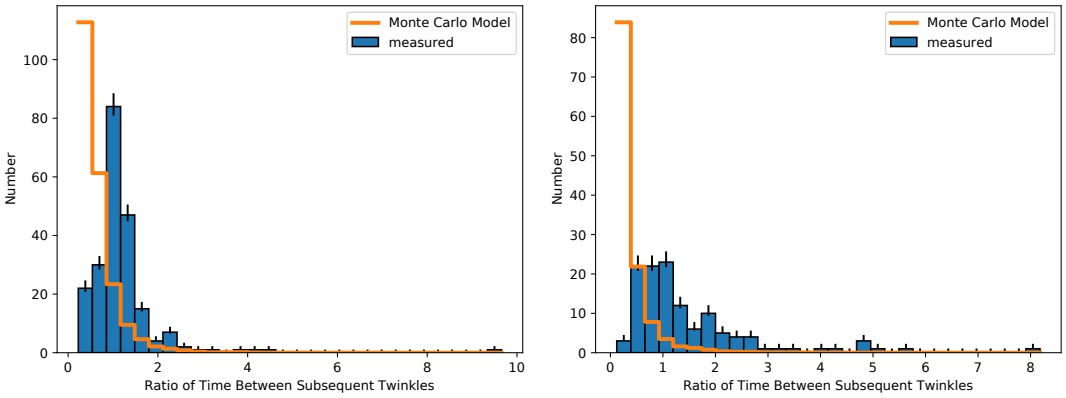

Figure 6. Histogram of the times between subsequent twinkles. Left is 2017, right is 2019 flashes.

There is a question of whether needles twinkle at a constant rate, or slow down. Saba et al. (2020) observed in optical that the time between subsequent twinkles tends to increase. In order to explore this we fitted the time of observed twinkles (T_i) with a simple model,

$$T_i = T_0 + i \times \Delta T \times f^{i-1} \,, \tag{1}$$

that has three parameters. T_0 is the time of the first twinkle. ΔT is the time between first two twinkles, and f is the twinkle-time increase factor. The twinkle-time increase factor determined if the time between twinkles was constant (if the best-fit f was 1), or increase over time (if the best-fit f is greater than 1). For each of the same set of needles used to generate the other distributions in this work we fitted this model to measured twinkle times using a Levenberg-Marquardt chi-squared minimizer. For calculating the chi-squared value we used 5% of the time between twinkles as the twinkle-time

error. We regularly miss twinkles from needles, which is easy to identify by eye when the separation between two twinkles is twice that between other twinkles in the same needle. Thus if very few twinkles were missed by our imaging, and it was clear by-eye which twinkles were missed, we allowed the model to include additional un-imaged twinkles as chosen by eye. However, if too many twinkles were missed by our imaging then that needle was excluded from fitting. The precise criterion used was that the number of un-imaged twinkles must be less-than or equal-to $N_{ot}-4$, where N_{ot} is the number of observed twinkles. In addition, negative leaders, recoil leaders, and the return stroke in the 2017 flash, affect needle activity (discussed in more detail in later sections). In this fitting we ignore the possible affects of negative leaders and recoil leaders. However, for the 2017 flash we only use needle twinkles that occur after the return stroke. Finally, we excluded needles that had a final chi-squared fit value greater than 6, which corresponds to 12% of the time between twinkles. In the 2017 flash we attempted to fit 46 needles. 21 were excluded because they had too few imaged twinkles after the return stroke, and two were excluded because the chi-squared fit was greater than 6. We attempted to fit 44 needles from the 2019 flash, 34 of which were excluded due to having too few imaged twinkles. All of the fitted needles from 2019 had a chi-squared less than 6.

The results of the fit for both flashes are shown in Figure 7, which shows the factor between subsequent twinkles vs the number of observed twinkles. The error bars are one-standard deviation error bars calculated from the analytical covariance matrix weighted by the resulting chi-squared fit value. For the 2017 flash all the needles from one particular leader are indicated. This is the same leader investigated in further detail in section 2.5 below. Figure 7 shows that some needles are consistent with a constant twinkling time (that is, the twinkle time factor is within three standard-deviations of 1.0), but there are also many needles that are not consistent with a constant twinkling time. No observed needles twinkle faster over time. The increase in twinkling time can be quite large, even over 30% increase per twinkle. The needles on one leader in the 2017 flash seem statistically consistent with having the same twinkle time factor, but it is difficult to do a detailed comparison of how nearby twinkles do or do-not relate to each other.

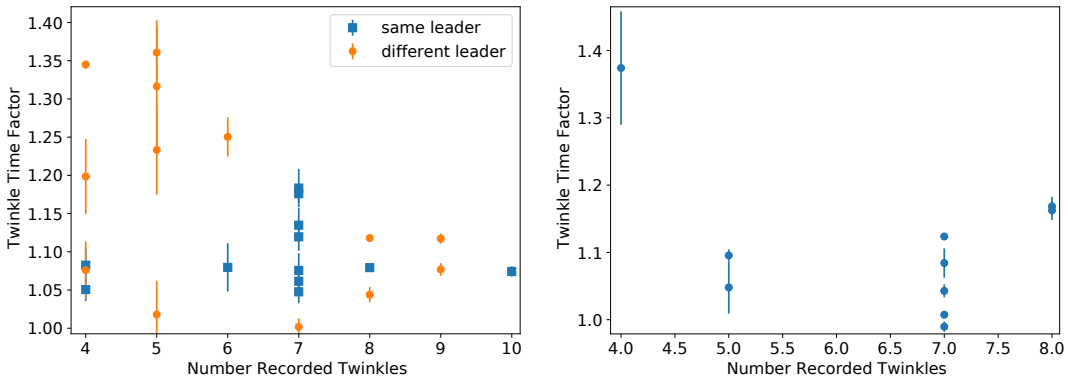

Figure 7. Fitted factor between subsequent twinkling times. Left is 2017, right is 2019 flashes.

Figure 8 shows the distribution of VHF needle lengths and Figure 9 shows the distribution of VHF lengths of individual twinkles divided by the length of the needle, for twinkles with more than one source. The length of each needle is the maximum distance along the fitted axis between any two sources in the needle, and the length of each twinkle is the maximum distance between any two sources in a twinkle. Thus, the VHF twinkle lengths can never be longer then a full VHF needle length. We'd like to emphasize that in this work we can only explore the length over which the twinkles and needles emit in VHF. It is always possible that a twinkle can propagate without emitting VHF, and thus is longer than what our measurements show. Later we will argue that this is probably common.

Figure 8 shows that while some needles can be relatively long (100-200 m), the vast majority are less than 40 m long with shorter needles occurring more often. Figure 9 shows that twinkles have relatively random VHF lengths relative to the total VHF length of the needle. The distribution of relative twinkle lengths for both flashes is statistically consistent with a uniform distribution (p-values of 0.48 and 0.20 respectively from a 1-sample Kolmagorov-Smirnov test).

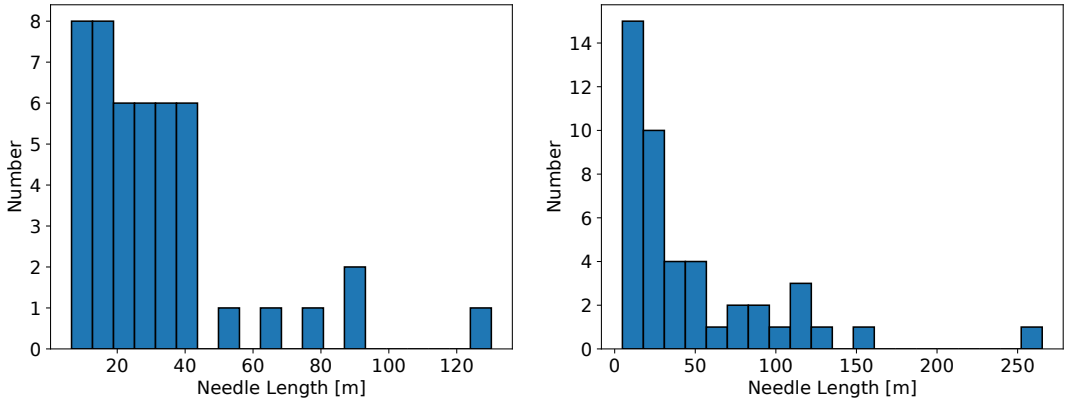

Figure 8. Length of each needle. Left is 2017, right is 2019 flashes.

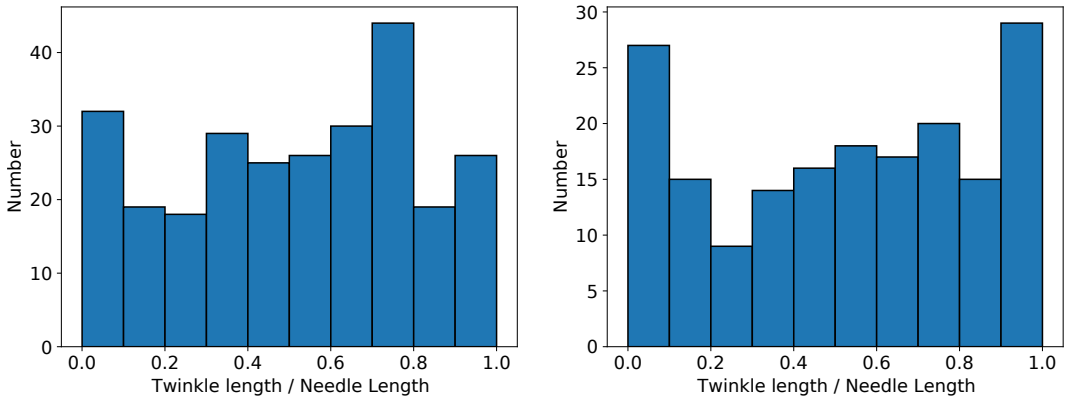

Figure 9. Histogram of length of each twinkle divided by the length of the needle, excluding twinkles of 1 source. Left is 2017, right is 2019 flashes.

Since, based on the needles shown in figure 2 and the distributions in figure 9, it is obvious that each twinkle does not emit mappable VHF over the whole length of the needle, we can explore the distributions of points where twinkles initially and finally emit VHF. Figure 10 shows the location, along the fitted axis, where each twinkle emits VHF closest to the base of the needle, divided by the VHF length of the needle, and figure 11 shows the VHF location farthest from the base of the needle, divided by the VHF length of the needle, for each twinkle. Figures 10 and 11 show that while twinkles tends to start and stop emitting VHF radiation closer to the base and tip of the needle, respectively, they can start and stop emitting VHF anywhere along the needle.

In order to show that twinkles, in general, do not extend the VHF length of a needle, figure 12 shows the difference between subsequent values from figure 11. That is, positive values in figure 12 means that a twinkle ended further along the needle than the previous twinkle, and negative values mean the previous twinkle ended closer to the base. The fact that the distributions in figure 12, for both years, are centered at zero, supports our observation that twinkles do not tend to extend the VHF length of a needle.

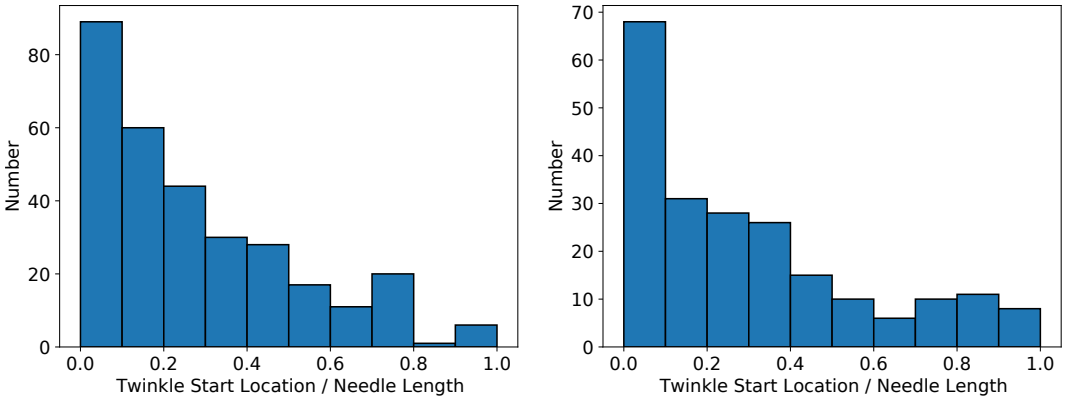

Figure 10. Histogram of the distance between the start of twinkles from the start of the needle, divided by the length of the needle. A '0' means the twinkle started near the beginning of the needle. A '1' means the twinkle started near the end of the needle (thus, the twinkle was necessarily short). Left is 2017, right is 2019 flashes.

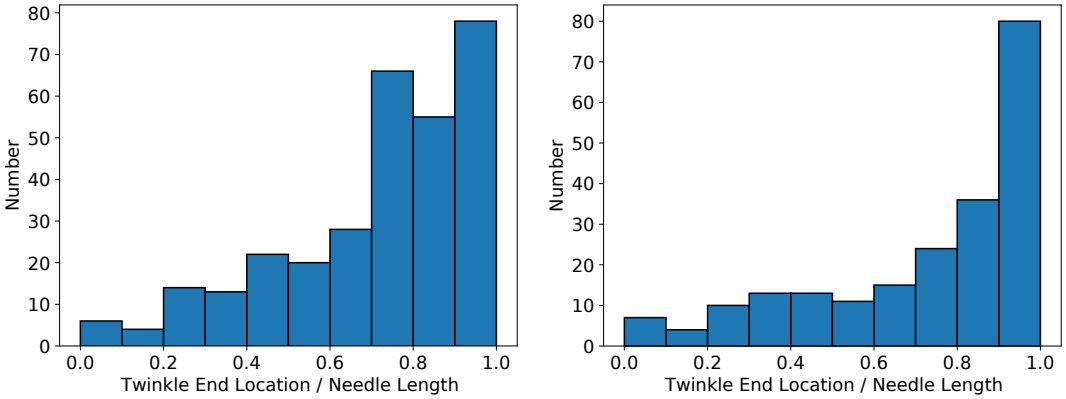

Figure 11. Histogram of the distance between the end of twinkles from the start of the needle, divided by the length of the needle. A '0' means the twinkle was short, and ended at the start of the needle. A '1' means the twinkle ended near the end of the needle (but does not imply the twinkle is long). Left is 2017, right is 2019 flashes.

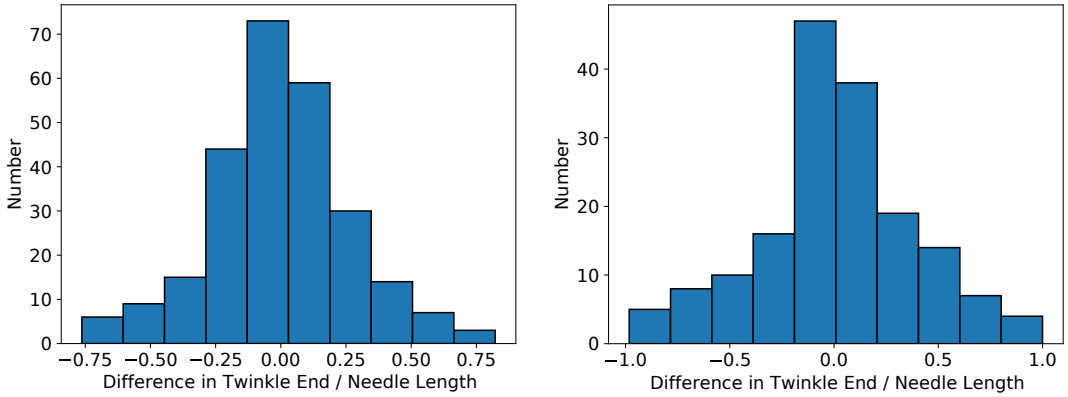

Figure 12. Histogram of the distance between the ends of subsequent twinkles, divided by the length of the needle. This is the difference between subsequent values from Figure 11. Left is 2017, right is 2019 flashes.

Figure 13 shows the distribution of distances between the VHF source locations and the fitted axis for each needle. Figure 13 essentially shows the VHF width of our needles. This distribution has a peak at 1-2 m from the needle axis, which is consistent with our location accuracy. That is, the needle widths are the same size as, or smaller than, our meter-scale location accuracy.

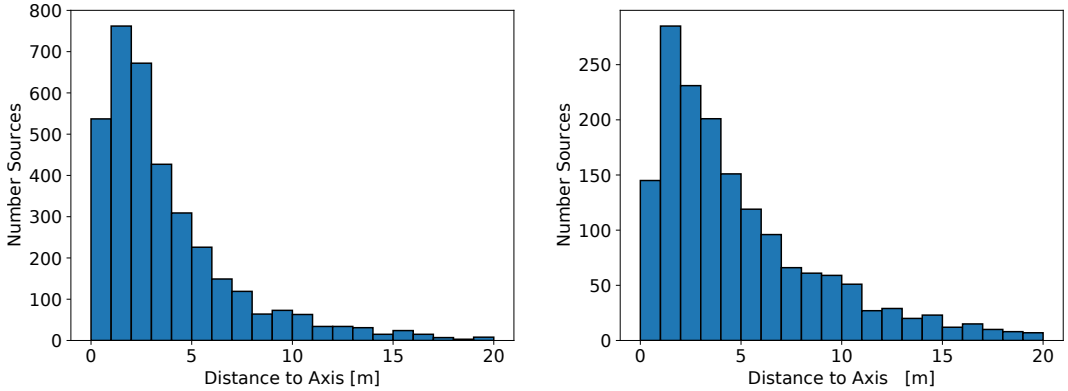

Figure 13. Distance from VHF sources in needles to the fitted axis. Left is 2017, right is 2019 flashes.

Figure 14 shows the distribution of twinkle propagation speeds found from the axis fitting discussed in section 2.1. The distributions in figure 14 only include twinkles that have more than 5 sources and the extracted standard error of the fitted speed was less

than 25% of the extracted speed. This distribution shows that twinkles have an extremely wide range of possible speeds. They can propagate as slow as a stepped leader (10^5 m/s), all the way up to the speed of a fast dart leader (10^7 m/s) (Dwyer & Uman, 2014). We have examined the fits of all twinkle speeds by eye, and while figure 16 shows the average speed of each twinkle, many twinkles are similar to those shown in figure 3 in that their propagation will start fast and slow down. Many other twinkles, however, maintain a constant propagation speed. Generating robust statistics for how often a twinkle slows down, however, is difficult and should be explored in future work.

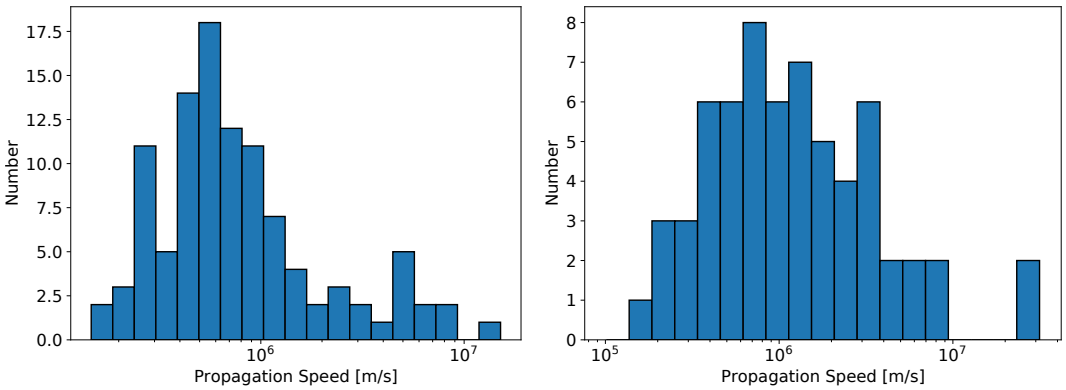

Figure 14. Speed of the twinkles. Left is 2017, right is 2019 flashes.

Figure 15 shows the VHF imaged source density versus twinkle propagation speed for each twinkle that we could calculate a speed for. The source density was simply the number of imaged sources divided by the VHF twinkle length. The 2017 flash has a very strong correlation between density and speed. The slower twinkles tended to have more sources per meter. The 2019 flash is similar, but the trend seems to be weaker. It is not clear if faster twinkles emit more VHF radiation, and so overwhelm the imager, or emit less VHF radiation.

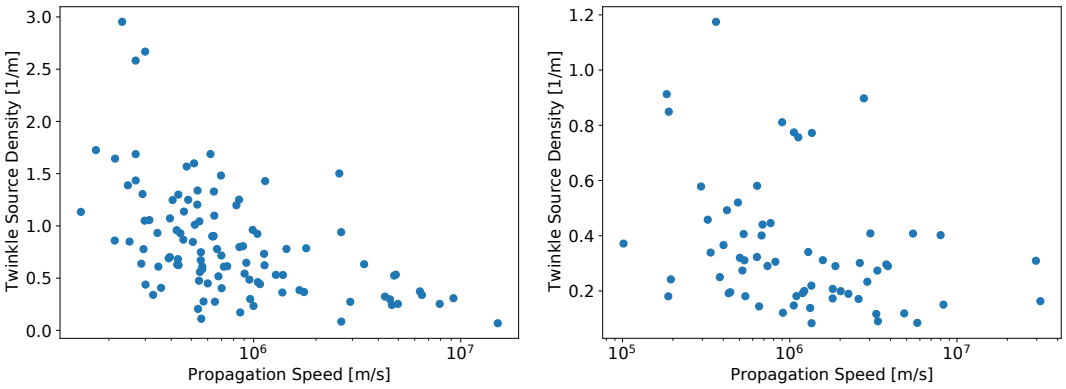

Figure 15. VHF source density per twinkle vs the speed of the twinkle. Left is 2017, right is 2019 flashes.

A close inspection of figure 2 shows that the VHF sources inside of each twinkle tend to cluster together. This is emphasized in figure 16, which shows the distribution of time between VHF sources inside of individual twinkles. If the VHF sources were scattered randomly in time then this distribution should be exponential, but instead we see a strong increase over an exponential at small time-differences. This is extremely similar to the VHF bursts we discussed in B. M. Hare et al. (2020), which we found along negative leaders, where we attributed the large peak at small time separation to stepping. This implies that needles, at least sometimes, tend to step like negative leaders.

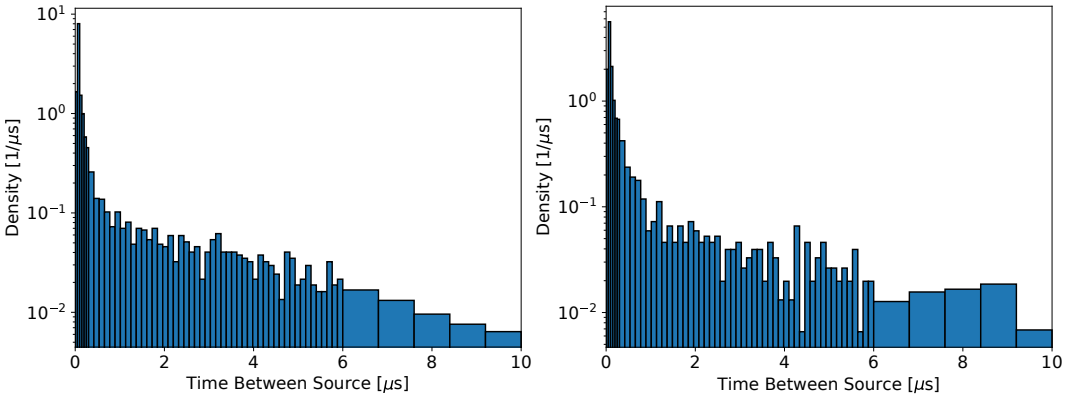

Figure 16. Distribution of time between sources in twinkles. Left is 2017, right is 2019 flashes.

Figure 17 shows the distributions of uncalibrated VHF pulse amplitudes from needles and negative leaders during the 2017 flash. These distributions were simply calculated by taking the amplitude of the associated VHF pulse on a reference antenna, squaring it and multiplying by distance to source squared. Similar to previous work, Figure 17 clearly shows that needles emit lower VHF power than negative leaders on average (Shao & Krehbiel, 1996; Li et al., 2020). However, unlike previous work, we have successfully separated needles and recoil leaders, and the distributions shown in figure 17 contain, at most, very few sources from recoil leaders. Figure 17 also appears to show that high-amplitude tail of VHF amplitude distributions have different shapes for negative and positive leaders, however, such subtleties need to be interpreted extremely carefully as figure 17 does not account for amplitude-dependent imaging efficiency.

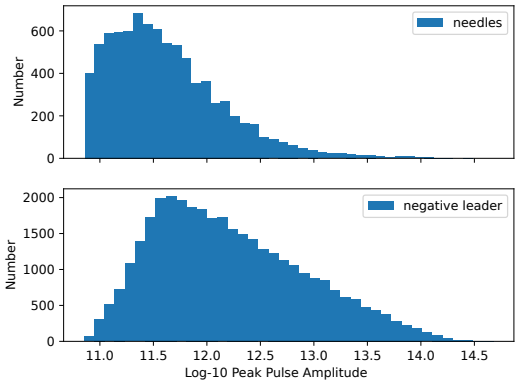

Figure 17. Distribution of VHF power emitted by needles and negative leaders during the 2017 flash.

2.3 Negative Stepped Leaders and Needles

Figure 18 shows a time slice of the 2017 and 2019 flashes, where in both flashes, a negative leaders terminates (at T=72 ms and T=115 ms for the 2017 and 2019 flashes respectively) and there is a period of 25 to 30 ms where there is no negative leader activity, then a new negative leader starts (at T=100 ms and T=137 ms in the 2017 and 2019 flashes respectively), as indicated in the figure. Figure 18 shows that during both flashes, when a new negative leader starts the needle activity is suppressed. However, this relationship is complex, as Figure 18 also clearly shows that needle activity seemed to increase as the negative leader in the 2017 flash approached ground, between times

t=60 ms to t=70 ms. This is a common feature we see in all imaged flashes, but we cannot exclude that possibility that it is at least partially due to the stronger VHF emissions from negative leaders masking the VHF emission from needles.

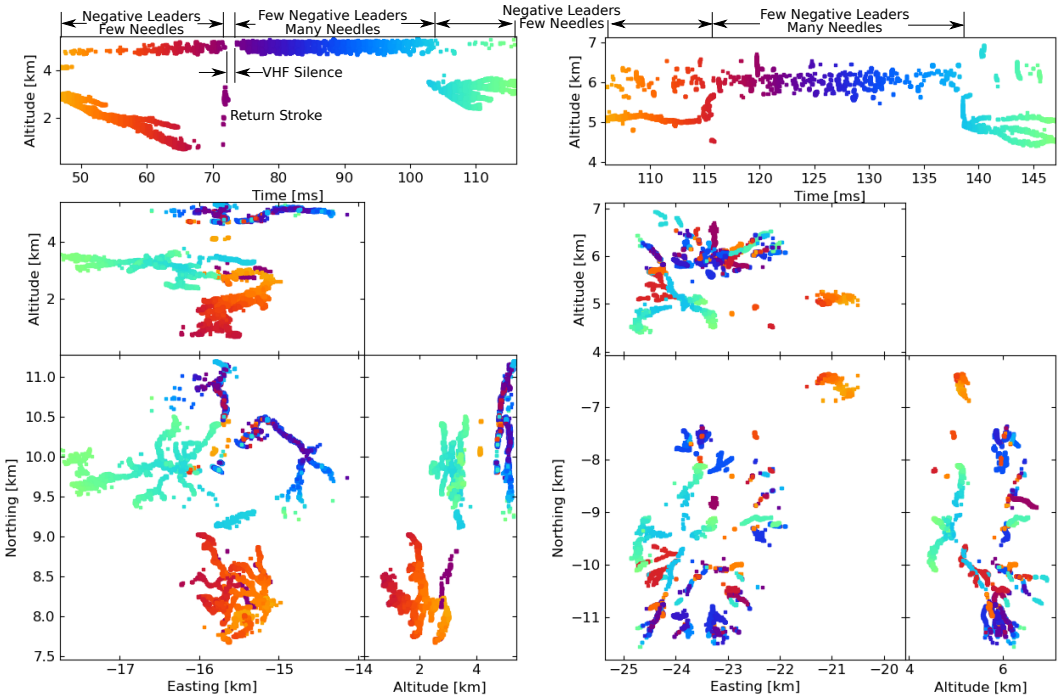

Figure 18. Relative relationship between negative leader and needle activity. Periods of negative leader activity and low needle activity, and vice-versa, is indicated. The return stroke and following period of VHF silence is also indicated for the 2017 flash. Left is 2017, right is 2019 flashes.

This suppression of needles, however, is not unique to negative leaders. The return stroke at T=72 ms in Figure 18 during the 2017 flash, seems to result in a large "hole" in needle activity following the return stroke. This lack of needles after the return stroke is not an imaging artifact, as we do not observe any VHF pulses from lightning above noise for about 1 ms after the return stroke. We have imaged one other flash with a return stroke, and it is ambiguous if that return stroke quenches needle activity or not. Further work is needed to explore the precise behavior of return strokes as imaged by LOFAR.

2.4 Recoil Leaders and Needles

The interactions between recoil leaders and needles are complex and varied. Here we report some of our observations on a few of the interactions we've observed. First, on rare occasion, we observe that a recoil leader will sometimes initiate a needle twinkle as it passes by the needle. One example is given in the appendix of B. Hare et al. (2019) shows the clearest example we've observed. The few other cases of recoil leaders inducing needle twinkles have not been nearly as clear.

We also regularly observe recoil leaders occurring at the same time that needles stop twinkling. Figure 19 shows a section of time during both flashes when there is significant recoil activity and very little negative leader propagation. The recoil leaders are clear in the Altitude vs Time panel as vertical bars and the needles appear as horizontal bands. This figure shows in both flashes a tendency of needles to build-up in intensity and then quench at the same time as a recoil leader, two examples are at T=198 ms in the 2017 flash and t=360 ms in the 2019 flash.

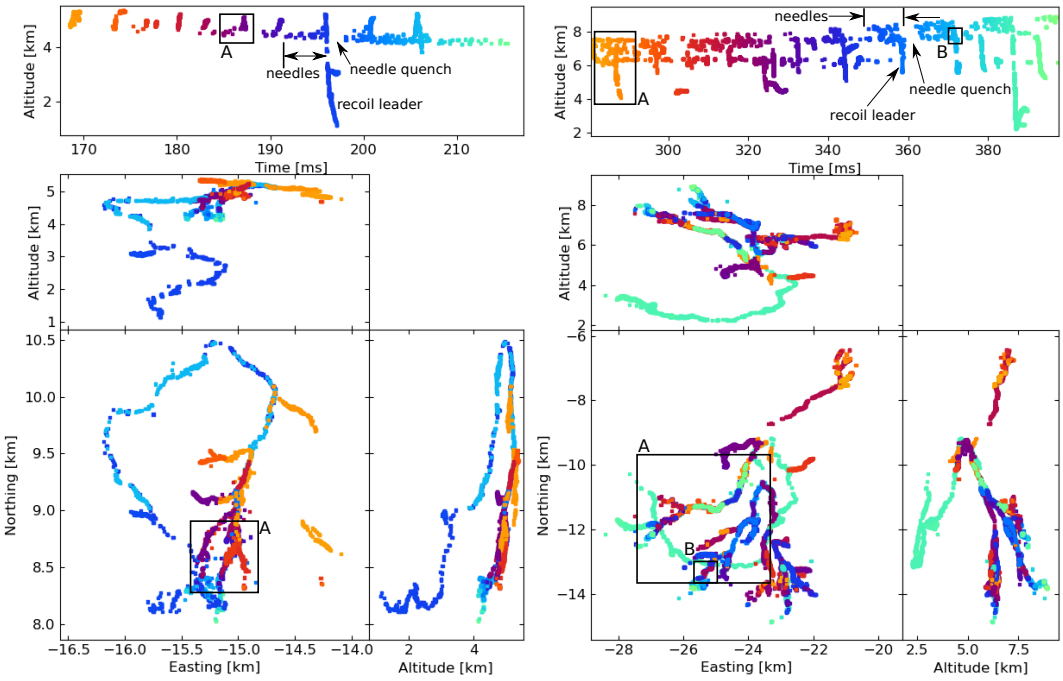

Figure 19. Relative relationship between recoil leader and needle activity. One group of needles, recoil leader, and period of needle silence is indicated for each flash. Rectangles labeled "A" for both flashed indicate the region focused-on in figure 20. The rectangles labeled "B" in the 2019 flash show the region focused-on in figure 21. Left is 2017, right is 2019 flashes.

Figure 20 shows a zoom in on a recoil leader from 2017 and 2019 that both occur at the same time that needle activity quenches. In both of these cases, and in many others, we see that the recoil leader starts farther up the leader branch (closer to the initiation-point of the flash) than the active needles, and the needles cease all activity for some time after the recoil leader. Needles on other leader branches, such as in the shown 2019 case, do not seem to be affected.

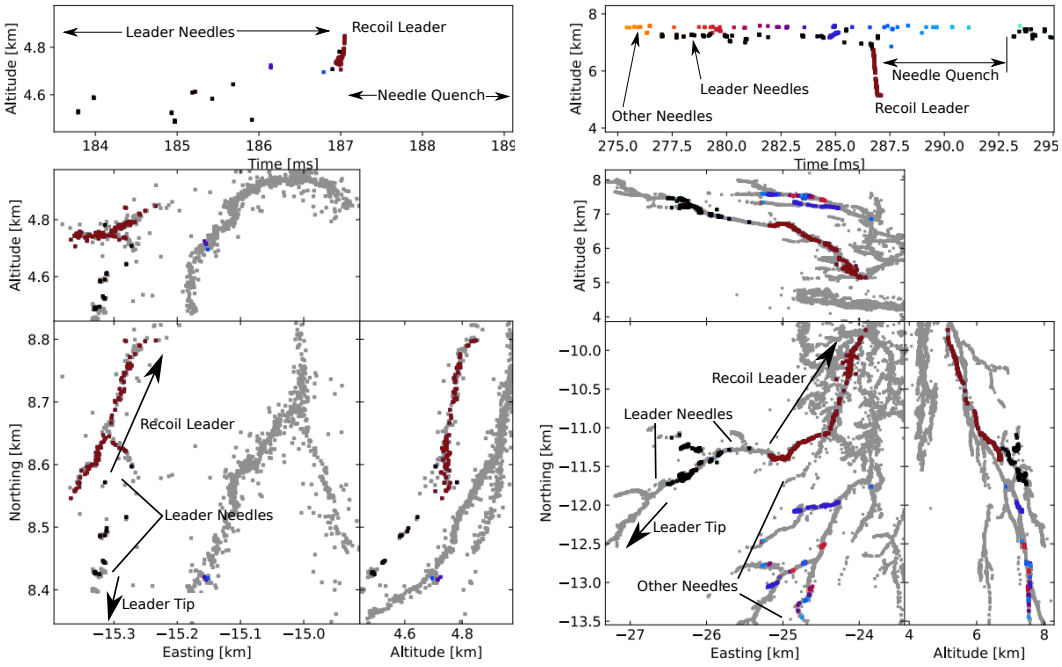

Figure 20. Two examples of a recoil leader occurring at the same time as a cessation of needle activity, as indicated by the rectangles labeled "A" in figure 19. Grey dots show all located VHF sources. Red dots show VHF sources from a recoil leader. Black dots show needle activity on the same leader branch as the recoil leader, and colored dots show needle activity from other leaders. The recoil leader and its direction, needles on the same leader (and different leader for 2019 flash), time period of needle quench, and general direction of leader tip is indicated. Left is 2017, right is 2019 flashes.

Of course, there are always variations from the standard scenario. Figure 21 shows an unusual case from 2019. This same recoil leader is shown in figure 19 at T=371 ms, in which this recoil leader appears similar to the others in that it occurs at the same time as a quenching of needle activity. However, a zoom-in to the beginning of the recoil leader, as in figure 21, shows that there was some kind of positive breakdown (shown in red) 400 μs

before the recoil leader. This positive breakdown reached 1×10^7 m/s in speed and occurred along a stretch of already-extent channel. This positive breakdown lead to an increase in needle activity over the channel that it propagated, and was then followed by a normal recoil leader, after which there was no needle activity on this branch for 4 ms.

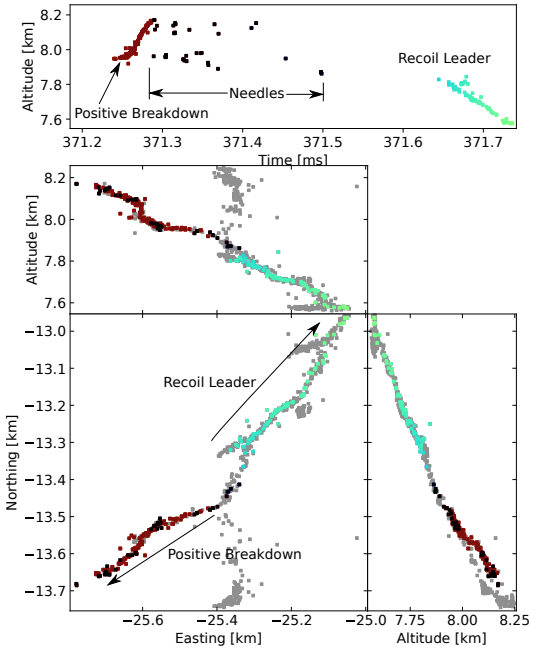

Figure 21. An example of an unusual event, from the 2019 flash. Red dots show some kind of positive breakdown. Black dots show needle activity, and colored dots show a recoil leader, also indicated by labels.

2.5 Needle Structure Along the Positive Leader

Top panel of figure 22 shows the distance of VHF sources along a positive leader channel of the 2017 flash vs their time. It was constructed by manually placing a linear spline over the path of the positive leader, choosing branches that propagated the furthest. Each source within a distance of 125 m from that spline is shown in the top panel of figure 22, at the time of occurrence and at the distance measured along the spline. The line in the top panel of figure 22 shows the location of the VHF source that is furthest along this leader branch. The bottom panel of figure 22 shows the histogram of all located sources (not just those along this branch), in order to compare the temporal density of needles to the temporal density of all located VHF sources. We choose a section of time before any significant recoil activity during the 2017 flash. We did not make a similar plot for

the 2019 flash due to amount of recoil activity. A similar figure was shown in Pu and Cummer (2019).

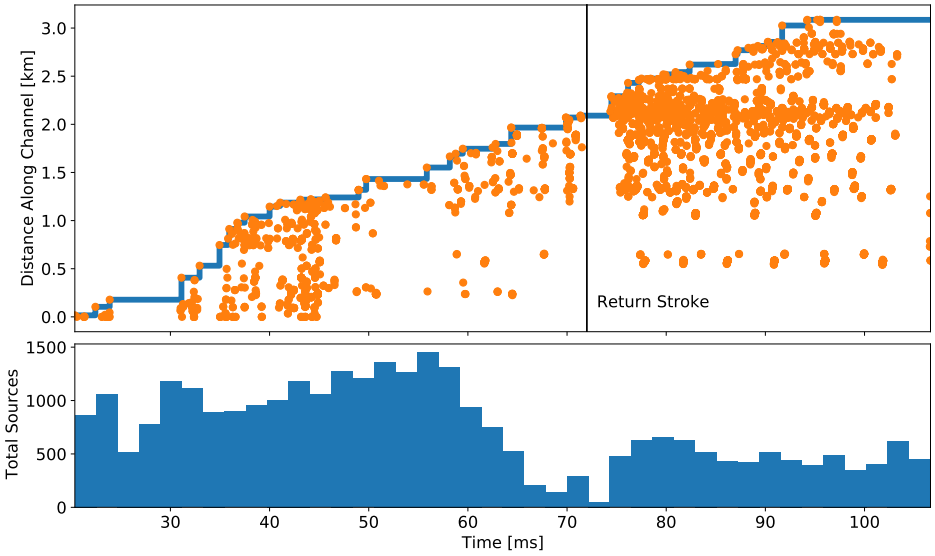

Figure 22. Top panel shows location vs. time of VHF sources along a positive leader channel of the 2017 flash. Colored line shows the distance of the source that is farthest along the positive channel. A vertical black bar shows the time of the return stroke. Lower panel shows histogram of all located sources (not just those on this leader).

Figure 22 shows that the density of needle activity over the leader is very non-uniform. As discussed previously, the observed needle activity is strongly anti-correlated with negative leader activity. For example, the imaged needle activity is highest after the return stroke, which is when there are fewest total VHF sources, as there were no propagating negative leaders between the return stroke and T=110 ms.

Similar to the findings of Pu and Cummer (2019), figure 22 shows that needles have a production head that propagates forward at about $5{\times}10^4$ m/s (Pu and Cummer (2019) measured 1×10^5 m/s and Saba et al. (2020) measured about 4×10^4 m/s, both projected in 2D), where all needle activity occurs behind this head. It is important to note that this head is not necessarily the location of the positive leader tip, as we cannot image the location of the positive leader tip in VHF. There are two ways we could infer a rough guess as to the distance between the needle front and the leader tip. First, is that the needle production front moves forward in jumps due to the discrete nature of nee-

dle activity. If the positive leader propagated smoothly, then the distance between the needle production front and negative leader cannot be much smaller than the distance the needle production front jumps forward. Figure 22 shows that these jumps are about 250 m long, and thus the distance between the needle production front and leader tip is most likely larger than 250 m. Secondly, at the beginning of the flash there is a period of about 15 ms between when we first observe the initial downward negative leader and the first needle activity. If we assume that the positive leader propagated during this time between 5×10^4-10×10^4 m/s, then the tip of the positive leader could be around 700-1,500 m in front of the needle production front. Saba et al. (2020) found that the tip of the positive leader was around 100-200 m in front of the needle activity for the upward positive leaders they observed. In contradiction with Pu and Cummer (2019), we find that needle activity occurs over a very long distance behind the needle front, with little to no decay in activity over distance. During the first 75 ms of the flash, the needle activity seems very continuous over the entire leader. After 80 ms the needles seem to twinkle over a 2.5-3.0 km length of channel.

Note that although there is a period of time with no needle activity after the return stroke, when the needle activity starts up again the needle production head moved forward by about 250 m, consistent with continuous silent propagation after the return stroke. Assuming that the tip of the positive leader maintains a relatively constant distance in front of the needle production head, this implies that the positive leader continued to propagate after the return stroke during the silent period of no received VHF signal.

Figure 23 is very similar to Figure 22, but only shows the needles in this region that were used in finding our statistical distributions discussed in previous sections. Figure 23 emphasizes the relationship between needles that are spatially close. Particularly, that twinkles of nearby needles are not correlated or anti-correlated. That is, we observe that twinkles that are spatially relatively close can twinkle at difference rates. A good example of this is two needles that are directly next to each other, shown in Figure 23 at a distance of about 0.5 km along the leader, after T=50 ms. These two needles seem to twinkle independently at different rates. This observation is precisely opposite to that made by Saba et al. (2020). Saba et al. (2020) seemed to observe that nearby needles twinkle out-of-phase with each other, which lead Saba et al. (2020) to hypothesize that needle twinkles could be due to some kind of wave that propagates down the channel. We believe that Saba et al. (2020) seemed to observe this behavior because they only

focused on a relatively small section of channel. If the needles twinkle at a regular rate, and the distance between needles is about equal to the speed of the leader times half the time between twinkles (which is the case in their data), then the twinkles from nearby needles will naturally appear to occur out-of-phase even if the needles have no interaction at all. Close examination of figure 3 in Saba et al. (2020) shows support not only for downward-going waves, but also equal evidence for upward-going waves, which strongly implies that downward-going twinkle-inducing waves are an observational artifact.

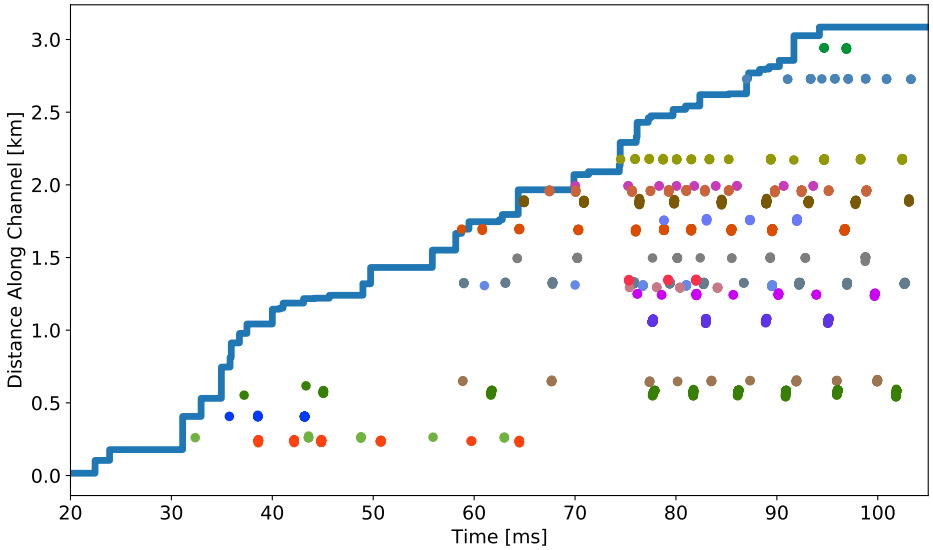

Figure 23. Location vs. time of VHF sources from selected needles along a positive leader channel of the 2017 flash. Colored line shows the distance of the source that is farthest along the positive channel.

3 Discussion

3.1 Field Reversal Mechanism

The fact that needles twinkle at a fairly regular rate that can decrease over time, neighboring needles can twinkle at different rates, each twinkle is a form of negative propagation, and that the twinkles propagate away from the positive leader, makes them difficult to explain. B. Hare et al. (2019) postulated that there must be an electric field reversal along the positive leader; where the tip of the positive leader has a outward-pointing electric field (as one would expect), but the electric field along the body of the positive leader points inward. B. Hare et al. (2019) further hypothesized that one possibility for

field reversal is if the positive leader became disconnected from the negative leader so that the positive leader would gain a more and more negative potential over time as it propagated, and needle twinkles would occur in order to equalize the potential between the leader and the ambient field around it. In this section we will thoroughly discuss the possibilities for how the electric field perpendicular to the leader channel could flip direction and point towards the channel. We will start with the simplest possible scenarios and gradually make the picture more realistic.

3.1.1 Channel disconnection without and with finite resistance

The first scenario we consider is the simplest case of a channel disconnection. That is, the leader channel is perfectly conducting and all the charge of the leader lies directly on the conducting leader (we ignore corona-sheath effects for the moment), and a perfectly insulating disconnection develops on the positive leader. In this scenario, diagrammed in figure 24, as the positive leader propagates in a uniform ambient electric field its electric potential will become more negative over time (since the electric field at the tip is roughly constant). Eventually, the later section of the positive leader (as shown in figure 24) will gain a more-negative potential than the ambient field. This will cause the electric field perpendicular to the later-half of the leader to point towards the channel, possibly inducing needle activity. Note that since we are only considering surface charge directly on the conducting leader, only the potential difference between the leader and the ambient field is important. As each needle twinkle neutralizes the electric field in its immediate vicinity, the amount of needle activity will be proportional to the rate of change of the leaders potential, and thus be uniform all along a section of leader that will grow in length at the same speed that the leader propagates. This prediction is very similar to what we observe in figure 22. This picture predicts a possibly large distance between the needle production front and the tip of the positive leader. As discussed in section 2.5, our data supports the possibility that there is about 750-1,500 m between the needle production front and leader tip, whereas Saba et al. (2020) observed there was only about 100-200 m between the leader tip and first needle activity.

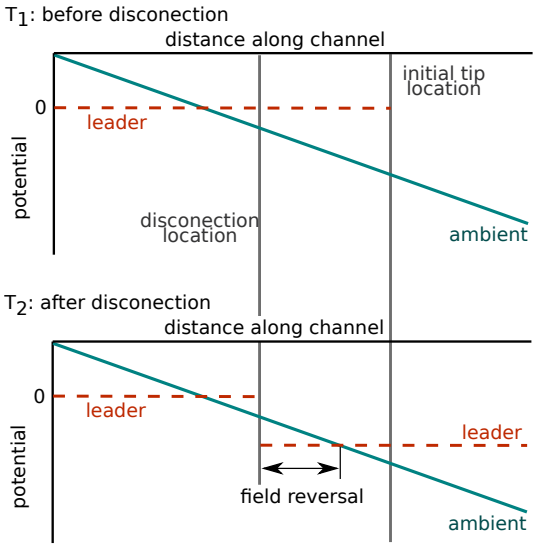

Figure 24. Most basic effects of leader disconnection. The ambient electric potential and leader potential are shown vs distance along the leader, before and after an insulating disconnection forms in the leader. A step-like discontinuity in the potential along the leader is shown due to the disconnection.

Next we consider the effect of resistance on the disconnection hypothesis. If the channel is not perfectly conducting and the break is not perfectly insulating then two changes from the basic picture will emerge.

1) The change in leader potential will not be a sharp discontinuity (as represented in figure 24), but will occur more smoothly in space.

2) Current will flow over the disconnection, thus the field-reversal will occur more slowly. The magnitude of the current will depend on the difference in potential across the leader (depending on how ohmic the leader channel is). In an extreme scenario, it is possible that the current across the disconnection could eventually equal the current injected into the positive leader by the propagating tip, in which case the potential will stabilize and shut down all needle activity on this leader. However, since the relationship between current and potential in a leader is not understood, it is not clear how quickly this effect will occur or if it will occur at all. it is even possible that the fact that this work and Saba et al. (2020) observes needle twinkling slowing down could be a result of this saturating field-reversal effect.

At first glance, this disconnection hypothesis seems to have two difficulties. First, needles have been observed on leaders that seem to be well conducting. Saba et al. (2020) observed needles on upward propagating leaders, and in this work we observe needle activity just before a return stroke that quenches the needle activity but does not show any VHF emission along the positive leader (thus implying that just before the return stroke there was some conducting connection between positive and negative leaders while the needles were active). Secondly, Pu and Cummer (2019) argues that the disconnection hypothesis predicts that needle activity should primarily occur around the disconnection which is contradictory with the observation of a needle-production front. However, as we have discussed, the disconnection hypothesis is still applicable when the positive leader channel carries current but is highly resistive, which could have been the case in Saba et al. (2020) and after the return stroke observed in this work. Furthermore, the disconnection hypothesis predicts needle activity over long lengths of positive leader channel where the channel has more negative potential than the ambient field, not just near the disconnection.

The disconnection hypothesis does precisely describe the interactions we observe between recoil leaders and needles as discussed in section 2.4, where we observe needle activity increases until a recoil leader occurs and quenches the needle activity because it equalizes the potential across the section. It seems that the recoil leaders quench needle activity because they reconnect the positive and negative leaders. After the recoil, the channel cools down until a portion of channel becomes highly resistive again, causing the needles to start twinkling again. Needle activity increases as the channel becomes more resistive until another recoil leader occurs.

3.1.2 Corona-sheath effect

Next we consider a more realistic situation with corona sheath charge. In this case it is possible for a field reversal to occur when the leader still has a more-positive potential than the ambient field. This corona sheath effect, as roughly detailed in figure 25, occurs when the leader charge density (charge on conductor plus charge in corona) at one spot leader becomes more negative over time. Note that it isn't necessary for the leader charge density to become negative in absolute terms. The result is that negative charge will accumulate on the surface of the conductor, inside of the still positive insulating corona sheath, producing an electric field that points towards the leader inside the

corona sheath and possibly outwards outside the corona sheath. This corona sheath effect could become important in two different situations.

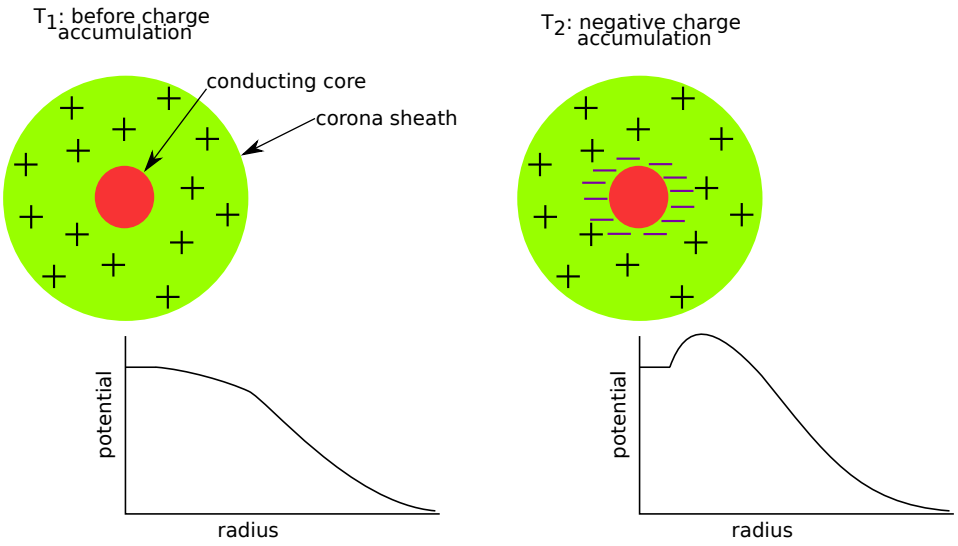

Figure 25. The corona sheath effect. Top portion shows the conducting core and corona sheath of the leader, and the positive charge density locked in the corona sheath. The bottom portion shows electric potential vs radius. The right side shows the difference if the total charge at this location becomes more negative, in which case negative charge could accumulate on the conducting leader and induce a more complex electric potential vs radius.

1) A leader at a uniform potential does not have a uniform charge density. That is, most of the charge is concentrated near the tip of the leader. Therefore, as illustrated in figure 26, a point on the positive leader starts its life at the tip of the positive leader with a large total charge density. But, as the leader propagates, the total charge density at them same point must decrease in order for the leader to maintain a constant potential. Via the corona sheath effect this could result in an electric field reversal just behind the tip of the leader. We refer to this as corona-induced field reversal. However, it is not clear how this mechanism could produce the observed repeated twinkling, as we would expect the first needle twinkle to discharge the corona sheath. Furthermore, this effect probably decays nearly exponentially behind the tip and so probably could not produce needle activity over 3 km of channel.

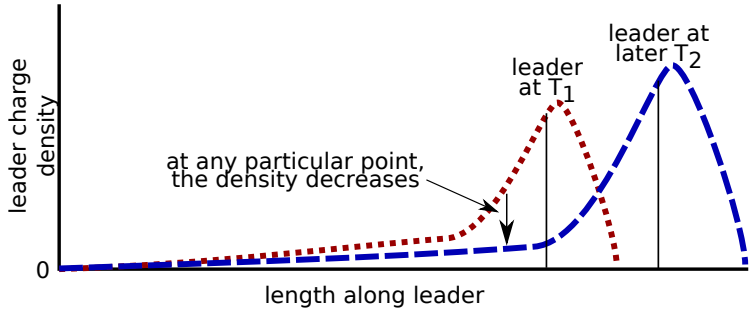

Figure 26. Propagation induced field reversal. While the total charge of a leader increases as it propagates, the total charge-density at any one spot must decrease, possibly leading to the corona-sheath affect.

2) The corona sheath effect will also enhance the field reversal due to a disconnection. Pu and Cummer (2019) predicted that this enhancement should occur mostly near the disconnection, as the negative charge density on the channel is highest near the disconnection. However, this is not correct. As discussed above, if the leader is well-conducting (except for the disconnection), then the field reversal due to a disconnection will be mostly constant along a long section of leader. Since the enhancement due to the corona sheath is proportional to the charge density in the corona, it will also be uniform along the positive leader (to the extent that the corona charge density is uniform). However, as illustrated in figure 26, the leader charge density far from the tip is probably quite small. Thus, it is entirely likely that the corona sheath near the disconnection could have already been discharged (possibly via needle activity), negating this effect.

In section 2.5 we observed that nearby needles can twinkle at different rates. Neither the disconnection hypothesis nor the corona-induced field reversal can explain this observation. It is possible that needles can alter the capacitance of the lightning channel, such that different needles require a different amount of charge before the perpendicular electric field is strong enough to initiate a twinkle.

3.2 Twinkle Propagation

One obvious question is, what is the nature of twinkle propagation? Do twinkles produce highly-conducting channels, like leaders, or not? Saba et al. (2020) clearly shows that needle twinkles have strong light emission, however, this does not necessarily im-

ply high conductivity (Malagón-Romero & Luque, 2019). In this work we have presented significant data pertaining to the nature of the propagation of twinkles. First, we have observed that needle twinkles have an extremely wide range of propagation speeds. Everywhere from 10^5 m/s up to and over 10^7 m/s, as shown in figure 14. The initial observation by B. Hare et al. (2019) missed this wide variety of speeds, probably because the fastest needles are more rare and they tend to have very few VHF sources. Figure 2 is a perfect example, as the 2017 twinkle at T=56 ms propagated at 1.5×10^7 m/s, but only had VHF sources at the base and tip of the needle and was not imaged in B. Hare et al. (2019). This wide distribution of propagation speeds strongly implies that needles have a wide variety of conductivity when they twinkle. Some needles are poorly conducting, and so the twinkle propagates slowly like a stepped leader, and some needles are more conducting and so the twinkles propagate more like recoil leaders. We have seen, in figure 3, that twinkles can slow down as they propagate. An obvious possible explanation is that the electric field decreases in amplitude further from the needle. If the corona sheath effect is significant than it is even possible that the electric field near the leader could point towards the leader, but at a further radial distance the electric field could point away from the channel again (as shown in figure 25) .

The hypothesis that needles have different temperatures when they twinkle, which results in a range of twinkle propagation behaviors, is consistent across all our observations. For example, in figure 2, it is clear that the different needle twinkles have different VHF source densities. Figure 15 shows that the imaged density of VHF sources weakly correlates with twinkle speed. Figures 10 and 11 show that twinkles do not all emit their first and last VHF sources in similar locations. This raises the distinct possibility that needle twinkles can propagate without emitting mappable VHF radiation. Furthermore, we have shown that needles have some tendency to step, as indicated by the distribution of time-differences between sources in figure 16. But, also needle twinkles have lower VHF amplitude on average then negative leaders, as shown by figure 17, which is consistent with the idea that needles remain warm between twinkles.

There seems to be a very strong limit on the length of needles, as we have observed very few longer than 100 m. The physical reason for this limit is not at all clear. Saba et al. (2020) showed that needles occur at the locations of corona-brush splits, and so we guess that the length of needles is related to the size of the corona at the tip of the leader, but such a hypothesis is very difficult to test.

3.3 The Silence of the Positive Leaders

B. Hare et al. (2019) noted that we are not able to image tip of the positive leader in VHF. The natural question that arises is, is it possible to set an upper limit on the VHF power emitted by the positive leader. In this work we noted that after the return stroke of the 2017 flash we did not receive any VHF radiation for almost a millisecond. Furthermore, after the return stroke the needle production front jumps forward by 250 m, consistent with continuous silent propagation of the positive leader. Thus, under the assumption that the positive leader was propagating during the VHF silence after the return stroke, the VHF power density emitted by a positive leader, at about 10 km distant, must be less than our background noise power, which is dominated by the galactic background, at about 1×10^{-12} W (B. M. Hare et al., 2020). Thus,

$$\frac{P_{Lemitted}}{R^2} A < P_{Grecived}\,, \tag{2}$$

where $P_{Lemitted}$ is the power emitted by the positive leader, R is the distance between the closest antenna and the positive leader ($\approx$ 8 km), A is the effective area of our antennas ($\approx$ 1 m^2), and $P_{Grecived}$ is the received galactic background power. Therefore, $P_{Lemitted} < 7{\times}10^{-5}$ W, in our 30-80 MHz frequency range, under our assumption that the positive leader was indeed propagating. For comparison, we have observed that the largest radio pulses we received from negative leaders have a peak power with an order-of-magnitude of 4 kW, emitted in 10 ns wide pulses of 40 μJ. Note here we discuss peak power, not average, since it is peak power that determines if we can see a VHF source without beam-forming.

4 Conclusions

In this work we have presented detailed observations of needles imaged in VHF. Including the distributions of times between twinkles, VHF lengths and twinkle propagation speeds. We have confirmed the observation of Saba et al. (2020) that the time between needle twinkles increases over time. Furthermore, we have observed that return strokes and recoil leaders can quench needle activity. It is also possible that negative leaders suppress needle activity, but it is not clear if this is an imaging artifact or not.

We have explored in detail possibilities for how the electric field perpendicular to the channel could reverse direction. We discussed the disconnection hypothesis, where if the positive leader becomes highly resistive than it could gain a more negative poten-

tial than the ambient field. This hypothesis describes the interactions between recoil leaders and needles very well, and could result in relatively uniform needle activity along the positive leader as is observed. We have also discussed the corona sheath effect, where negative charge accumulation on the leader channel can result in a complex field configuration, included field reversal close to the channel. This will happen behind the tip of a propagating leader, which we call corona-induced field reversal. Corona-induced field reversal can explain needle activity on well conducting leader channels, but it only results in needle activity very close to the leader tip.

We have concluded that because needle twinkles have such a wide variety of speeds and VHF structure, then they likely have a wide variety of propagation mechanisms, ranging from twinkles that act like step leaders up to twinkles that propagate like dart leaders. This implies the strong possibility that needle twinkles can propagate without emitting VHF, and that this range of phenomena is due to the temperature of the needle at the time of each twinkle.

Acknowledgments

The LOFAR cosmic-ray key science project acknowledges funding from an Advanced Grant of the European Research Council (FP/2007-2013) / ERC Grant Agreement n. 227610. The project has also received funding from the European Research Council (ERC) under the European Unions Horizon 2020 research and innovation programme (grant agreement No 640130). We furthermore acknowledge financial support from FOM, (FOM-project 12PR304). ST acknowledges funding from the Khalifa University Startup grant (project code 8474000237). BMH is supported by NWO (VI.VENI.192.071). KM is supported by FWO (FWO-12ZD920N). AN acknowledges the DFG grant NE 2031/2-1. TNGT acknowledges funding from the Vietnam National Foundation for Science and Technology Development (NAFOSTED) under [Grant number 103.01-2019.378]. LOFAR, the Low Frequency Array designed and constructed by ASTRON, has facilities in several countries, that are owned by various parties (each with their own funding sources), and that are collectively operated by the International LOFAR Telescope foundation under a joint scientific policy.

The data are available from the LOFAR LTA, see `https://www.astron.nl/lofarwiki/doku.php?id=public:lta_howto` (section "Staging Transient buffer Board (TBB) data") for access. The file names of the two flashes are:

L612746_D20170929T202255.000Z_"stat"_R000_tbb.h5 and

L703974_D20190424T194432.504Z_"stat"_R000_tbb.h5. Both must have the prefix:

srm://srm.grid.sara.nl/pnfs/grid.sara.nl/data/lofar/ops/TBB/lightning/ and "stat" should be replaced with the station name: CS001, CS002 CS003, CS004, CS005, CS006, CS007, CS011, CS013, C017, CS021, CS024, CS026, CS028, CS030, CS031, CS032, CS101, CS104, RS106, CS201, RS205, RS208, RS210, CS301, CS302, RS305, RS306, RS307, RS310, CS401, RS406, RS407, RS409, CS501, RS503, RS508, or RS509.

References

Dwyer, J. R., & Uman, M. A. (2014). The physics of lightning. *Physics Reports*, *534*(4), 147 - 241. (The Physics of Lightning) doi: 10.1016/j.physrep.2013.09.004

Edens, H. E., Eack, K. B., Eastvedt, E. M., Trueblood, J. J., Winn, W. P., Krehbiel, P. R., ... Thomas, R. J. (2012). Vhf lightning mapping observations of a triggered lightning flash. *Geophysical Research Letters*, *39*(19). doi: 10.1029/2012GL053666

Hare, B., et al. (2019). Needle-like structures discovered on positively charged lightning branches. *Nature*, *568*, 360363. doi: 10.1038/s41586-019-1086-6

Hare, B. M., Scholten, O., Dwyer, J., Ebert, U., Nijdam, S., Bonardi, A., ... Winchen, T. (2020, Mar). Radio emission reveals inner meter-scale structure of negative lightning leader steps. *Phys. Rev. Lett.*, *124*, 105101. Retrieved from `https://link.aps.org/doi/10.1103/PhysRevLett.124.105101` doi: 10.1103/PhysRevLett.124.105101

Li, S., Qiu, S., Shi, L., & Li, Y. (2020). Broadband vhf observations of two natural positive cloud-to-ground lightning flashes. *Geophysical Research Letters*, *47*(11), e2019GL086915. Retrieved from `https://agupubs.onlinelibrary.wiley.com/doi/abs/10.1029/2019GL086915` (e2019GL086915 2019GL086915) doi: 10.1029/2019GL086915

Malagón-Romero, A., & Luque, A. (2019). Spontaneous emergence of space stems

ahead of negative leaders in lightning and long sparks. *Geophysical Research Letters*, *46*(7), 4029-4038. Retrieved from `https://agupubs.onlinelibrary.wiley.com/doi/abs/10.1029/2019GL082063` doi: 10.1029/2019GL082063

Pu, Y., & Cummer, S. A. (2019). Needles and lightning leader dynamics imaged with 100-200 mhz broadband vhf interferometry. *Geophysical Research Letters*, *46*(22), 13556-13563. doi: 10.1029/2019GL085635

Saba, M., de Paiva, A., & Concollato, L. (2020). Optical observation of needles in upward lightning flashes. *Scientific Reports*, *10*, 17460. doi: 10.1038/s41598-020-74597-6

Scholten, O., Hare, B., Dwyer, J., Sterpka, C., Kolmaov, O., I.and Santolk, Ln, R., ... Winchen, T. (2020). The initial stage of cloud lightning imaged in high-resolution. *submitted to JGR:Atmospheres*. doi: 10.1002/essoar.10503153.1

Shao, X. M., & Krehbiel, P. R. (1996). The spatial and temporal development of intracloud lightning. *Journal of Geophysical Research: Atmospheres*, *101*(D21), 26641-26668. doi: 10.1029/96JD01803

Shao, X. M., Rhodes, C. T., & Holden, D. N. (1999). Rf radiation observations of positive cloud-to-ground flashes. *Journal of Geophysical Research: Atmospheres*, *104*(D8), 9601-9608. doi: 10.1029/1999JD900036

van Haarlem, M. P., et al. (2013). LOFAR: The LOw-Frequency ARray. *A&A*, *556*, A2. doi: 10.1051/0004-6361/201220873